

General Disclaimer

One or more of the Following Statements may affect this Document

- This document has been reproduced from the best copy furnished by the organizational source. It is being released in the interest of making available as much information as possible.
- This document may contain data, which exceeds the sheet parameters. It was furnished in this condition by the organizational source and is the best copy available.
- This document may contain tone-on-tone or color graphs, charts and/or pictures, which have been reproduced in black and white.
- This document is paginated as submitted by the original source.
- Portions of this document are not fully legible due to the historical nature of some of the material. However, it is the best reproduction available from the original submission.

IT RELEASE

213
n Facility

NO

NASA

NATIONAL AERONAUTICS AND SPACE ADMINISTRATION

MSC INTERNAL NOTE NO. 68-FM-120

May 21, 1968

CSM-ACTIVE RENDEZVOUS SIMULATION
STUDIES USING SEXTANT AND
RANGING DEVICE

By B. F. Cockrell,
Mathematical Physics Branch



MISSION PLANNING AND ANALYSIS DIVISION

MANNED SPACECRAFT CENTER
HOUSTON, TEXAS

FACILITY FORM 602

N70-35844
(ACCESSION NUMBER)

(THRU)

15
(PAGES)

1
(CODE)

TMX-64469
(NASA CR OR TMX OR AD NUMBER)

21
(CATEGORY)

MSC INTERNAL NOTE NO. 68-FM-120

PROJECT APOLLO

CSM-ACTIVE RENDEZVOUS SIMULATION STUDIES
USING SEXTANT AND RANGING DEVICE

By B. F. Cockrell
Mathematical Physics Branch

May 21, 1968

MISSION PLANNING AND ANALYSIS DIVISION
NATIONAL AERONAUTICS AND SPACE ADMINISTRATION
MANNED SPACECRAFT CENTER
HOUSTON, TEXAS

Approved: 
James C. McPherson, Chief
Mathematical Physics Branch

Approved: 
John P. Mayer, Chief
Mission Planning and Analysis Division

CONTENTS

Section	Page
SUMMARY	1
INTRODUCTORY.	1
ANALYSIS AND RESULTS.	2
The Simulation Method	2
Study A	2
Study B	3
Study C	3
CONCLUSIONS	4
REFERENCES.	12

TABLES

Table		Page
I	INSTRUMENT ERROR MODEL	
	(a) Noise 1σ	5
	(b) Bias	5
	(c) IMU misalignment	5
II	RELATIVE STATE ERRORS OBTAINED FROM CSI TO TPF USING BOTH A VHF RANGING DEVICE AND SEXTANT FOR A CSM- ACTIVE LUNAR RENDEZVOUS	6
III	ERRORS AT THE BEGINNING OF TRACKING AND AT CDH FOR VARIOUS COMBINATIONS OF SIGNS ON THE INITIAL CM STATE VECTOR.	7
IV	STANDARD DEVIATIONS OF THE RELATIVE STATE VECTOR ERRORS AT CSI AND CDH FOR THE VALUES IN TABLE III.	9

CSM-ACTIVE RENDEZVOUS SIMULATION STUDIES

USING SEXTANT AND RANGING DEVICE

By B. F. Cockrell

SUMMARY

This report presents and discusses the results of three lo studies designed to simulate onboard navigation for a CSM-active LM rescue in lunar orbit. The results show that the CM lunar rendezvous navigation system, which is a combination of the sextant and ranging device, will satisfactorily support LM rescue navigation.

INTRODUCTION

The primary mode of rendezvous for the lunar landing mission is one in which the lunar module is the active vehicle as it maneuvers to intercept the command and service modules. If, after the LM ascent and insertion, the LM should become immobilized, the CSM must then become the active rendezvous vehicle and effect an LM rescue. Since the CSM does not have a rendezvous radar, as does the LM, it must utilize its 28-power sextant and an independent very high frequency (VHF) ranging device to update the onboard-computed state vectors necessary to accomplish the rendezvous.

Three separate studies are presented in this document:

Study A - Comparison of navigation performance for various instruments - sextant, rendezvous radar, and sextant and the independent VHF ranging device - during the concentric sequence initialization (CSI) to constant differential height (CDH) phase of the LM rescue.

Study B - Study of navigation performance when the VHF ranging device and sextant are used for LM rescue from CSI to terminal phase-finalization (TPF).

Study C - Study comparing various initial errors possible from a given covariance matrix.

ANALYSIS AND RESULTS

The Simulation Method

The simulation program used is described in detail in reference 1. Basically the method is as follows. First, nominal trajectories are generated for each vehicle using an accurate numerical integration program. For the LM, the trajectory was generated in one piece since the vehicle is "dead". The CSM trajectory, however, was generated piecewise (i.e., from burn to burn assuming nominal burns). From these two trajectories, shaft, trunnion, and range observations were generated. The processing of observations by the Apollo CM guidance computer (CMC) is accomplished by the measurement incorporation routine (section 5.2.3, ref. 2). At the time a measurement is made, the best estimate of the state vector of the spacecraft is the extrapolated estimate containing the six components of position and velocity. The extrapolation of the vehicle's state vector is accomplished by the Encke technique. This approach requires numerical integration of the disturbing accelerations only. The actual position and velocity are the sums of the two-body conic state and these disturbing deviations. From this state vector estimate it is possible to determine an estimate of the quantity measured. When the predicted value of this measurement is compared with the actual measured quantity, a difference, the residual, is generated.

A weighting vector is computed from statistical knowledge of state vector uncertainties and tracking performance and a geometry vector determined by the type of measurement being made. The weighting vector is defined such that a statistically optimum linear estimate of the deviation from the estimated state vector is obtained when the weighting vector is multiplied by the residual.

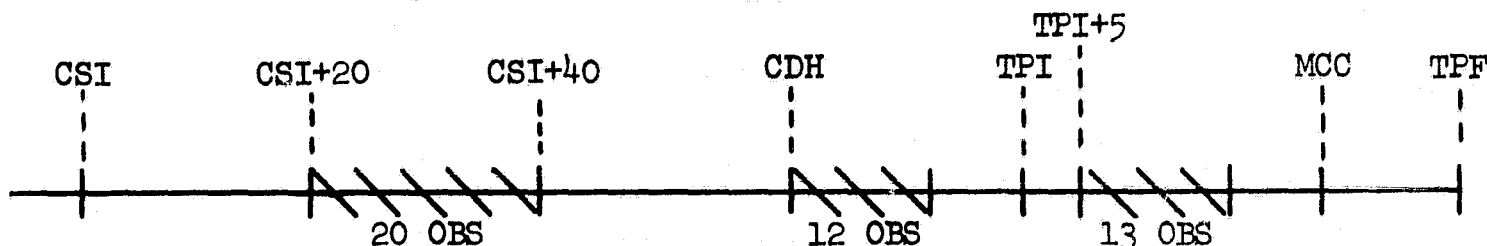
Study A

The comparison of navigation instruments is presented in figures 1(a) and (b). All four cases (the fourth case being no navigation) had the same initial errors, initial covariance matrix, observation profile and observation frequency (1 per minute). The profile represents the CSI to CDH phase of a CSM-active LM rescue. The tracking begins at CSI + 20 minutes with a relative state error (CSM-LM) of 79 559 ft in position magnitude and 58 fps in velocity magnitude. The initial covariance matrix in each case was a 6×6 diagonal with 1000 ft as values for the position components and 1 fps for the velocity components. This matrix represents to the on-board filter, the state uncertainties in relative position and velocity; that is, the diagonal is the weight given to the state vector since the Kalman filter assumes that the state is part of the observation set. Observations were taken at the rate of 1 per minute for 20 minutes and the state uncertainty was then propagated to the time of the CDH burn. The instrument error model is described in table I.

The results of the study are presented in figure 1. The study shows that the addition of an independent VHF ranging device, when used with the sextant, greatly enhances navigation accuracy for the problem studied. In fact, the state errors remaining after tracking and propagation indicate that the VHF position determination ability is 14 times better than the sextant, 5 times better than the rendezvous radar, and 20 times better than nothing at all. For velocity errors (which are indicative of fuel costs) the results are even more startling. The VHF velocity errors are 18 times better than the sextant, 6 times better than rendezvous radar, and 24 times better than no navigation.

Study B

The study of the navigation performance of the CM navigation system for lunar operations was established as part of the MPAD RCS fuel cost study for CSM-active rendezvous in LM rescue operations. After having shown that the VHF ranging device was capable of supporting one phase of rendezvous (CSI to CDH) the next step was to expand the investigation through all phases of the LM rescue. In the study the instrument error model is the same as that described for the VHF ranging device and sextant combination in study A. The tracking profile was



The results of this study are presented in table II. An important thing to note is the ability of the VHF ranging device and sextant to handle different types of velocity errors. This is important in fuel studies. In the first tracking interval the instruments reduced a 67.12-fps altitude velocity error to less than 3 fps. In the second interval the initial error was 9.77 fps out of plane and the VHF ranging device and sextant reduced this error to essentially zero. In the entire navigation sequence from CSI to TPF the VHF and sextant reduced a position error of 11.9 n. mi. to 81 ft and a velocity error of 68.87 fps to 0.05 fps.

Study C

The errors in the initial conditions for simulation studies can be determined from a covariance matrix which describes the initial state vector uncertainties. The method used in this study to select the errors from the covariance matrix was to take the square root of the diagonal of the covariance matrix for the magnitude of the errors. The signs of the errors can be determined from the cross correlations of the elements.

of the vector if the cross correlations are sufficiently high. All possibilities of direction can be covered by studying the possible combinations of sign on the errors.

In this study it was assumed that only the out-of-plane errors were well-known. The diagonal of a statistically produced covariance matrix was taken to be a six-dimensional vector representing the error in orbit plane coordinates of the relative (CSM to LM) state. As stated above the out-of-plane errors (w, \dot{w}) in both position and velocity were assumed small. The other components of this error vector (u, v, \dot{u}, \dot{v}) were assumed to be well known in magnitude only. The possibilities of direction for a six-dimensional vector given two known components are 16. These sixteen sets of errors were added to the relative state at CSI and then propagated for 20 minutes. Beginning at this point twenty observations were taken with the VHF and sextant at 1 per minute. The error at end of tracking was then propagated to the time of the CDH maneuver. The magnitudes of the initial error vector were

$$\begin{aligned}\delta u &= 20\ 301.46\ \text{ft} \\ \delta v &= 20\ 484.13\ \text{ft} \\ \delta w &= 2\ 691.05\ \text{ft} \\ \delta \dot{u} &= 23.74\ \text{fps} \\ \delta \dot{v} &= 11.28\ \text{fps} \\ \delta \dot{w} &= 2.32\ \text{fps}\end{aligned}$$

The errors at beginning of track and at CDH are presented in table III; the standard deviations of the errors in table III are given in table IV. The VHF ranging device and sextant error models are the same as those on page 5. It is interesting to note that the standard deviation in position and velocity errors at CDH was 691 ft and 0.5 fps, respectively. This means that, for the size errors given, the VHF ranging device and sextant can determine relative errors to well within tolerable limits no matter what direction the errors take. However, this is not true for the sextant alone.

CONCLUSIONS

This study demonstrates that a combination of sextant angles and VHF range measurements comprises the most effective onboard navigation system yet investigated for the Apollo spacecraft. Unlike the effectiveness of the sextant alone, the effectiveness of the combination is independent of the distribution of initial uncertainty. This capability is especially significant in fuel consumption studies since velocity uncertainty can be reduced to less than 1 fps.

TABLE I.- INSTRUMENT ERROR MODEL

(a) Noise 1σ

Instrument	Range	Shaft, m.rad.	Trunnion, m.rad.	Range rate
Rendezvous radar	$(1/3)\%$ of range	0.332	0.283	$(\frac{1.3}{3})\%$ of RR
Sextant	--	0.2	0.2	--
VHF and sextant	80 ft	0.2	0.2	--

(b) Bias

Instrument	Range, ft	Shaft, m.rad.	Trunnion, m.rad.	Range rate, fps
Rendezvous radar	167	-1.13	2.42	1/3
Sextant	--	0.2	0.2	--
VHF and sextant	1	0.2	0.2	--

(c) IMU misalignment

CSM, m.rad. per axis (for sextant and VHF and sextant observations) 0.2

LM, m.rad. per axis (for RR observations) 1.0

Drift, deg per hour per axis (both platforms) 0.03

TABLE II.- RELATIVE STATE ERRORS OBTAINED FROM CSI TO TPF
 USING BOTH A VHF RANGING DEVICE AND SEXTANT FOR A
 CSM-ACTIVE LUNAR RENDEZVOUS

Event	Time, min from CSI	Position errors, ft	Velocity errors, fps	Component errors				$\Delta \dot{V}$, fps	$\Delta \dot{W}$, fps
				ΔU , ft	ΔV , ft	ΔW , ft	$\Delta \dot{U}$, fps		
Begin track CSI + 20	20	81 373	68.87	21 438.59	-78 427.56	3 329.66	67.12	-12.33	-9.25
End track CDH	39	934	1.65	802.21	-369.32	302.75	1.55	-.57	-.024
	59	3 159	3.05	1 533.56	-2 760.65	106.68	2.77	-1.25	-.27
Begin track CDH	60	3 255	9.77	103.45	-84.99	3 252.63	.098	-.064	-9.77
End track TPI	71	168	.15	11.56	-111.25	124.98	-.11	-.058	-.086
	81	365	.52	338.36	12.39	176.15	.51	.054	-.0017
Begin track TPI + 5	86	565	.78	532.50	-136.82	128.87	.76	-.13	-.042
End track	98	94	.11	-35.67	-85.74	11.09	-.0046	-.093	.059
MCC	107	65	.07	15.08	-34.86	53.09	.027	-.029	.559
TPF	124	81	.05	22.32	-54.96	54.57	.032	-.035	.025

9

TABLE III.- ERRORS AT THE BEGINNING OF TRACKING AND AT
CDH FOR VARIOUS COMBINATIONS OF SIGNS ON THE INITIAL CM STATE ERRORS

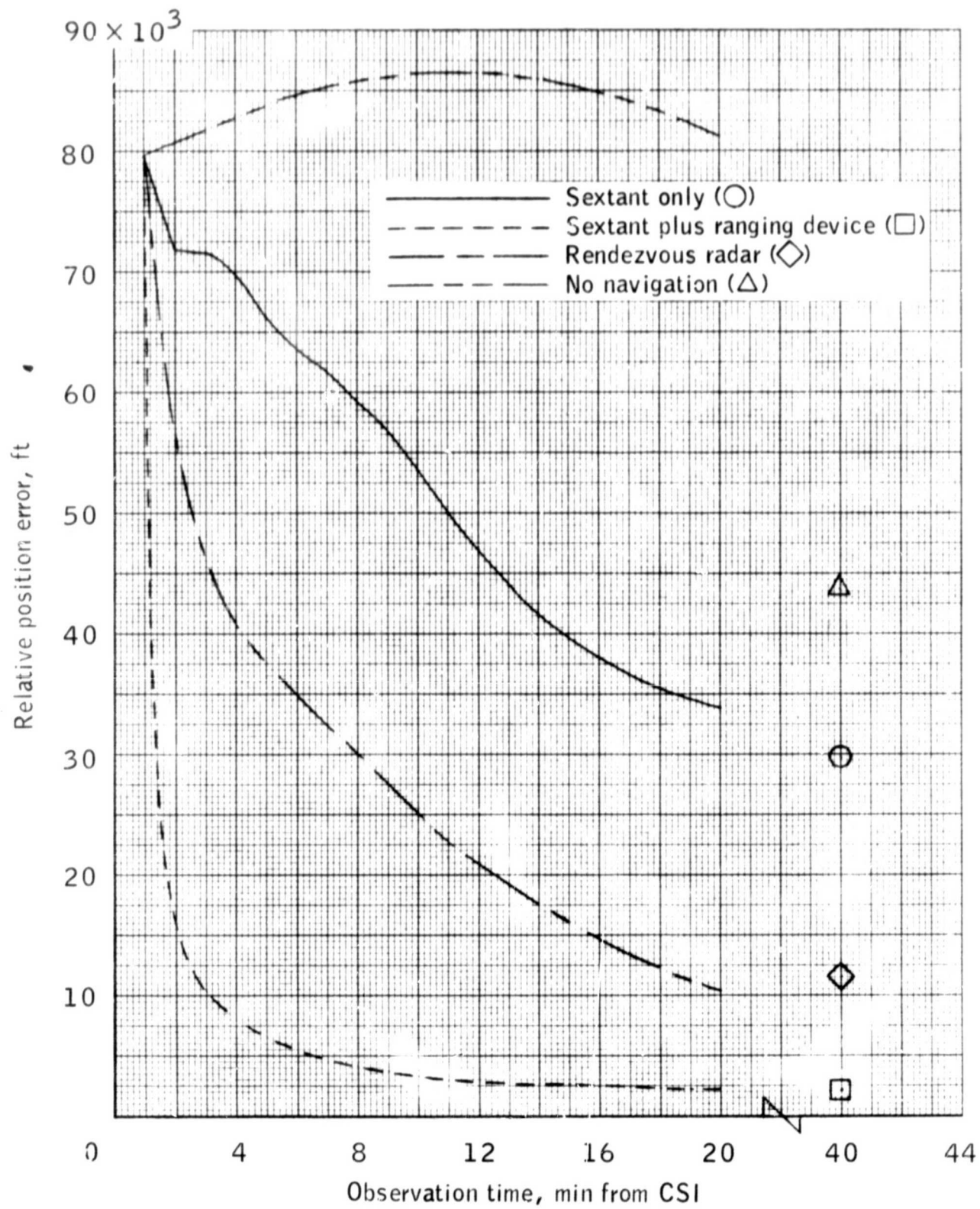
Event	Position errors, ft	Velocity errors, fps	Component errors			
			ΔU , ft	ΔV , ft	$\Delta \dot{U}$, fps	$\Delta \dot{V}$, fps
CSI + 20	15 139	27.20	3 207	-14 351	-2.90	27.00
CDH	1 438	1.68	1 000	-1 016	1.58	-.500
CSI + 20	45 020	40.40	22 731	-38 693	38.20	-13.00
CDH	2 374	2.39	1 255	-2 009	2.20	-.920
CSI + 20	25 406	19.00	-3 327	-24 928	-15.80	10.50
CDH	1 405	1.65	995	-974	1.60	-.49
CSI + 20	40 721	51.10	29 212	-28 143	51.00	3.40
CDH	2 605	2.59	1 336	-2 231	2.40	-1.0
CSI + 20	25 367	19.10	3 545	24 860	15.80	-10.70
CDH	1 354	1.57	935	-961	1.50	-.47
CSI + 20	44 976	40.40	-22 249	38 921	-38.10	13.30
CDH	2 036	1.68	706	-1 904	1.50	-.78
CSI + 20	40 721	51.30	-28 990	28 369	-51.20	-3.20
CDH	2 083	1.67	676	-1 966	1.40	-.79
CSI + 20	15 108	27.30	-3 143	14 334	2.80	-27.20
CDH	1 355	1.57	926	-926	1.50	-.48

TABLE III.- ERRORS AT THE BEGINNING OF TRACKING AND AT
CDH FOR VARIOUS COMBINATIONS OF SIGNS ON THE INITIAL CM STATE ERRORS - Concluded

Event	Position errors, ft	Velocity errors, fps	Component errors			
			ΔU , ft	ΔV , ft	$\dot{\Delta U}$, fps	$\dot{\Delta V}$, fps
CSI + 20	28 555	8.3	-23 657	-15 580	-2.25	-7.98
CDH	1 460	1.62	919	-1 119	1.51	-.53
CSI + 20	44 119	54.2	-43 036	9 019	-43.5	32.3
CDH	2 291	1.67	589	-2 210	1.41	-.86
CSI + 20	18 159	13.6	-17 086	-4 986	10.6	8.5
CDH	1 447	1.62	931	-1 092	1.51	-.52
CSI + 20	49 817	58.7	-49 659	-1 602	-56.5	15.8
CDH	2 341	1.66	556	-2 270	1.38	-.88
CSI + 20	28 580	8.5	23 733	15 514	2.22	8.16
CDH	1 262	1.79	1 031	-1 199	1.67	-.58
CSI + 20	44 028	53.7	42 987	-8 819	43.1	-32.0
CDH	3 229	3.14	1 586	-2 810	2.85	-1.28
CSI + 20	49 742	58.1	49 585	1 664	55.97	-15.58
CDH	3 591	3.47	1 739	-3 147	3.15	-1.43
CSI + 20	18 156	13.6	17 083	5 005	-10.7	-8.3
CDH	1 513	1.73	1 014	-1 108	1.6	-.54

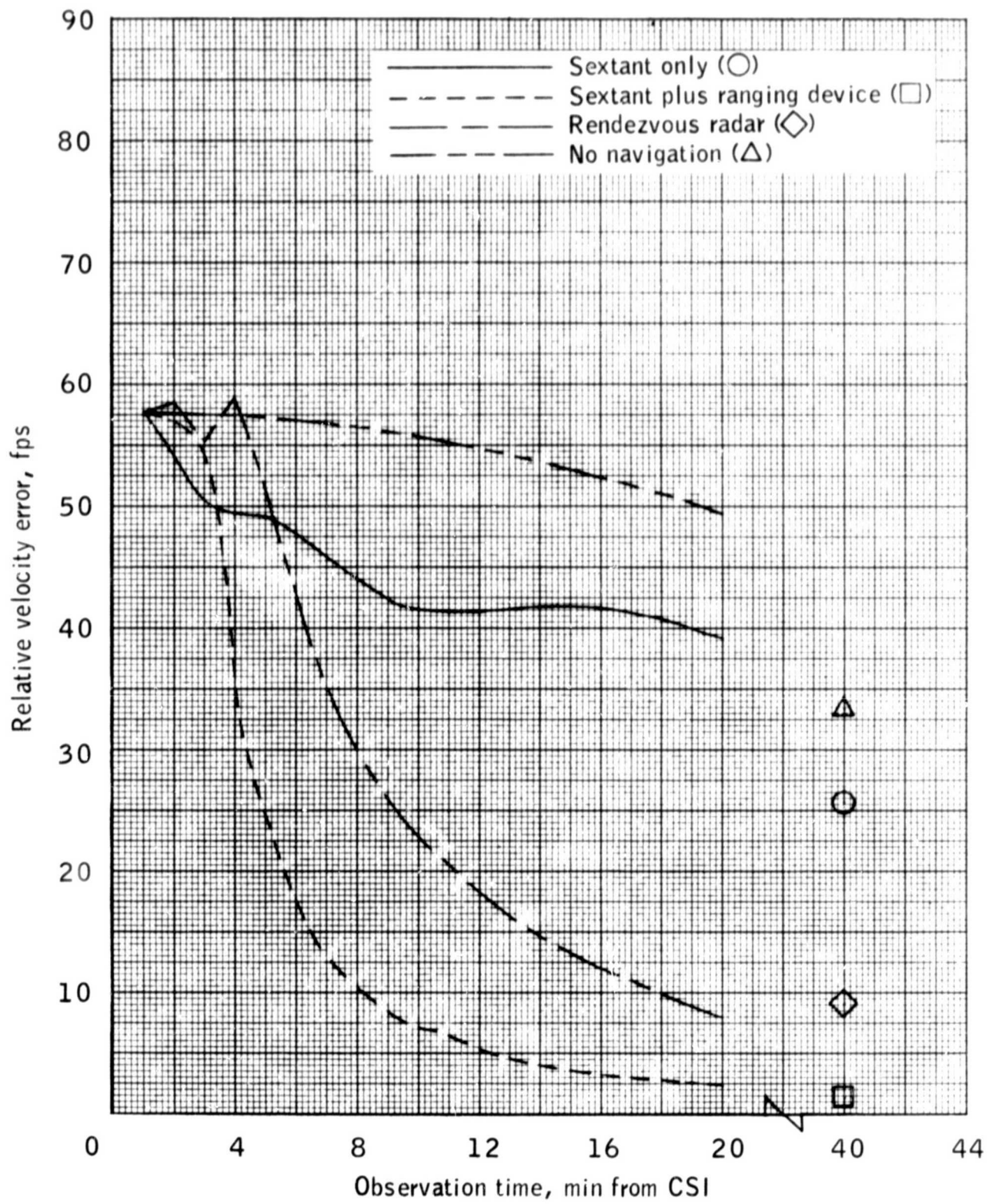
TABLE IV.- STANDARD DEVIATIONS OF THE RELATIVE
STATE VECTOR ERRORS AT CSI AND CDH FOR THE VALUES IN TABLE III

Event	Position errors, ft	Velocity errors, fps	Component errors			
			ΔU , ft	ΔV , ft	$\Delta \dot{U}$, fps	$\Delta \dot{V}$, fps
STD DEV AT CSI + 20	12 370	18.30	28 592	20 852	34.4	17.4
STD DEV AT CDH	691	.58	321	697	.7	.4



(a) Relative position error.

Figure 1.- Navigation comparison for relative position and velocity errors before CDH.



(b) Relative velocity error.

Figure 1.- Concluded.

REFERENCES

1. Clifford, J. B., Jr: Apollo Coasting Flight Navigation Simulation - OBSIM/NAVSIM Program Formulation. TRW Note No. 67-FMT-531, July 25, 1967.
2. Colossus GSOP Section 5 (R-577), MIT, December 1967.